Supporting Materials

Text 1. Existing ML-based wetland CH_4 upscaling products

(Peltola et al., 2019) upscaled monthly CH_4 fluxes for the Arctic-boreal freshwater wetland in 2013-3014 at 0.25°-0.5° spatial resolution with three temporal variables including MODIS LST at night, snow cover, and potential radiation, as well as a static binary permafrost map. The training data composed 488 monthly data records from 25 EC tower sites, spanning 2005-2016.

(McNicol et al., 2023) upscaled monthly CH_4 fluxes for global freshwater wetland in 2001-2018 at 0.25° with air temperature (with and without a 2-week lag), MODIS EVI with a 3-week lag, mean temperature of the driest quarter, precipitation of the wettest month, and vegetation canopy height (Simard et al., 2011). Meteorological data was from WorldClim (Fick & Hijmans, 2017). The training data consisted of 6,210 weekly observations between 2006 and 2018 acquired from 43 EC sites.

Text 2. Tower EC flux data

The base of our EC data collection stems from a publicly available global synthesis coordination of FLUXNET-CH_4, which includes 79 EC tower sites (42 are freshwater wetland sites) and 293 site-years of data. We collected both daily and half-hourly data from 44 sites in the Arctic-boreal region (>45° N), accounting for 167 site years as our base dataset, to which we added data from 6 new sites (31 site-years) and added additional data to 9 existing sites (21 site-years) contributed by site PIs (Table S2). In total, we assembled data from 50 EC tower sites in northern latitudes (219 site-years), of which 33 are from wetlands (155 site-years), with 13 wet tundra sites, 11 fens, and 9 bogs. Data entries with missing data in gridded predictors were excluded, including 5 wetland sites (FI-LOM, DE-SFN, RU-SAM, RU-VRK, SE-ST1) where data was collected before SMAP data was available. Another 2 sites (CA-BOU, RU-COK) were excluded after quality control. After quality filtering, data from 26 wetland sites were used for analysis (Table S2).

Half-hourly data obtained from FLUXNET-CH_4 were gap-filled following the FLUXNET protocols (Pastorello et al., 2020). Specifically, for CH_4 fluxes (FCH_4), the FLUXNET-CH_4 gap-filling procedure includes filling gaps in meteorological variables with ERA-Interim reanalysis data and then gap-filling FCH_4 using artificial neural networks (ANN) (Knox et al., 2019). Variables used to gap-fill FCH_4 included air temperature (TA), downward-incoming shortwave radiation (SWin), wind speed (WS), air pressure (PA), and sine and cosine functions to represent seasonality. For the sites with additional half-hourly data that we assembled in this study, we used the same predictors to fill gaps in FCH_4 except for gap-filling meteorological variables with ERA5 data. We used RF algorithm as it can fill gaps within 12 days with low normalized MAE for fens and bogs (Irvin et al., 2021). The R^2 of gap-filling models across sites ranged 0.35-0.89 (mean R^2 = 0.68).

The 33 wetland sites accounted for 74% of the daily EC tower data after quality control. The remaining 26% data consisted of 17 non-wetland sites, including upland forests, meadows, dry tundra, pasture, and lakes (Table S2).

Text 3. Bottom-up and top-down models

The bottom-up estimates we used for comparison were from sixteen wetland CH_4 models in the Global Carbon Project (GCP) Methane Budget (Z. Zhang et al., 2023). We calculated the mean annual and mean seasonal emissions and uncertainties for the study area from the model diagnostic simulations using a gridded climate data set from Climate Research Unit (CRU) as the inputs. The maximum and minimum estimations in each year were identified as the upper and lower bounds of the uncertainty range. Mean annual and mean seasonal emissions were also calculated from 18 extensive WetCHARTs models, with the maximum and minimum values representing the range of uncertainties.

The top-down inversions were from the atmospheric methane assimilation system, CarbonTracker-CH_4, which can simulate monthly CH_4 emitted to the atmosphere attributed to microbial, fossil, and pyrogenic sources at 2° x 3° resolution (Bruhwiler et al., 2014). In the high latitudes, microbial emissions mainly consist of natural wetland and open water emissions, and ruminant and wild animal emissions.

Text 4. ML algorithms comparison

Many studies have endorsed random forest as outperforming other machine learning algorithms in gap-filling and upscaling CH_4 fluxes (Irvin et al., 2021; Kim et al., 2020; C. Zhang et al., 2020). We tested ANN and SVM with the same dataset we used to build the ensemble random forest models. Results indicate that random forest models outperformed ANN and SVM in these wetlands with higher R^2 and lower MAE and RMSE (Fig. S8). The ability of random forest to handle highly nonlinear problems supports upscaling the temporally highly varied and spatially heterogeneous CH_4 fluxes. Random forest can incorporate continuous, discontinuous, and categorical variables. Properly tuned random forest models can avoid overfitting and may capture nonlinear and discontinuous signals in environmental variables (Kim et al., 2020), such as soil moisture, to better model daily variability in CH_4 fluxes.

Text 5. Model predictive performance at sites

We examined 9 EC sites where model predictive performance was below median performance metrics (1 bog, 2 fen, and 6 wet tundra sites). The R^2 between the upscaled fluxes and observations at a fen site (US-BZF) and 3 wet tundra sites (RU-CHE, US-ATQ, US-BEO) were significantly improved compared to the predictive performance at these sites when they were taken out of training, indicating the unique patterns in these sites. Drainage is observed in US-

BZF and RU-CHE (Kwon et al., 2022). JJA and SON season fluxes at CA-PB1, US-ATQ, US-NGC sites were overestimated, where US-ATQ contains sandy soils (Wang et al., 2022) and CA-PB1 is drier compared to a sedge-dominated peatland site CA-PB2 (Humphreys et al., 2021).

RU-CHE and RU-CH2 are two Chersky sites in East Siberian Russia about 600m apart from each other to form a paired disturbance experiment. RU-CH2 is a control tower over an undisturbed wetland, whereas RU-CHE is a tower affected by artificial drainage. The above-ground conditions of the two sites are virtually identical, but soil temperature and moisture are different. Drainage caused lower CH_4 fluxes at RU-CHE compared to those at RU-CH2 (Fig. S7). However, the grid-level input could not discern the soil conditions at both sites due to coarser spatial resolution, resulting in low model predictive performance at the RU-CHE site.

US-Los is a small wetland where previous work has shown that water-table depth and shortwave radiation covary and are good predictors of methane fluxes (Burdun et al., 2023). Half-hourly air temperature is also correlated with diurnal methane fluxes, with some component of methanogenesis likely transported via lateral aquatic fluxes (Reed et al., 2018). The wetland is associated with the presence of glacial till affecting its elevation, and thus elevation is found to be a good predictor of methane emissions at local scales.

References:

Bruhwiler, L., Dlugokencky, E., Masarie, K., Ishizawa, M., Andrews, A., Miller, J., Sweeney, C., Tans, P., & Worthy, D. (2014). CarbonTracker-CH_4: An assimilation system for estimating emissions of atmospheric methane. *Atmospheric Chemistry and Physics*, *14*(16), 8269–8293. https://doi.org/10.5194/acp-14-8269-2014

Burdun, I., Bechtold, M., Aurela, M., De Lannoy, G., Desai, A. R., Humphreys, E., Kareksela, S., Komisarenko, V., Liimatainen, M., Marttila, H., Minkkinen, K., Nilsson, M. B., Ojanen, P., Salko, S.-S., Tuittila, E.-S., Uuemaa, E., & Rautiainen, M. (2023). Hidden becomes clear: Optical remote sensing of vegetation reveals water table dynamics in northern peatlands. *Remote Sensing of Environment*, *296*, 113736. https://doi.org/10.1016/j.rse.2023.113736

Fick, S. E., & Hijmans, R. J. (2017). WorldClim 2: New 1-km spatial resolution climate surfaces for global land areas. *International Journal of Climatology*, *37*(12), 4302–4315. https://doi.org/10.1002/joc.5086

Humphreys, E., Bieniada, A., & Todd, A. (2021). *An analysis of methane emissions from four peatland sites in the Hudson Bay Lowlands*. *2021*, B32E-02. https://ui.adsabs.harvard.edu/abs/2021AGUFM.B32E..02H

Irvin, J., Zhou, S., McNicol, G., Lu, F., Liu, V., Fluet-Chouinard, E., Ouyang, Z., Knox, S. H., Lucas-Moffat, A., Trotta, C., Papale, D., Vitale, D., Mammarella, I., Alekseychik, P., Aurela, M., Avati, A., Baldocchi, D., Bansal, S., Bohrer, G., … Jackson, R. B. (2021). Gap-filling eddy covariance methane fluxes: Comparison of machine learning model predictions and uncertainties at FLUXNET-CH4 wetlands. *Agricultural and Forest Meteorology*, *308–309*, 108528. https://doi.org/10.1016/j.agrformet.2021.108528

Kim, Y., Johnson, M. S., Knox, S. H., Black, T. A., Dalmagro, H. J., Kang, M., Kim, J., & Baldocchi, D. (2020). Gap-filling approaches for eddy covariance methane fluxes: A comparison of three machine learning algorithms and a traditional method with principal component analysis. *Global Change Biology*, *26*(3), 1499–1518. https://doi.org/10.1111/gcb.14845

Knox, S. H., Jackson, R. B., Poulter, B., McNicol, G., Fluet-Chouinard, E., Zhang, Z., Hugelius, G., Bousquet, P., Canadell, J. G., Saunois, M., Papale, D., Chu, H., Keenan, T. F., Baldocchi, D., Torn, M. S., Mammarella, I., Trotta, C., Aurela, M., Bohrer, G., … Zona, D. (2019). FLUXNET-CH4 Synthesis Activity: Objectives, Observations, and Future Directions. *Bulletin of the American Meteorological Society*, *100*(12), 2607–2632. https://doi.org/10.1175/BAMS-D-18-0268.1

Kwon, M. J., Ballantyne, A., Ciais, P., Qiu, C., Salmon, E., Raoult, N., Guenet, B., Göckede, M., Euskirchen, E. S., Nykänen, H., Schuur, E. A. G., Turetsky, M. R., Dieleman, C. M., Kane, E. S., & Zona, D. (2022). Lowering water table reduces carbon sink strength and carbon stocks in northern peatlands. *Global Change Biology*, *28*(22), 6752–6770. https://doi.org/10.1111/gcb.16394

McNicol, G., Fluet-Chouinard, E., Ouyang, Z., Knox, S., Zhang, Z., Aalto, T., Bansal, S., Chang, K.-Y., Chen, M., Delwiche, K., Feron, S., Goeckede, M., Liu, J., Malhotra, A., Melton, J. R., Riley, W., Vargas, R., Yuan, K., Ying, Q., … Jackson, R. B. (2023). Upscaling Wetland Methane Emissions From the FLUXNET-CH4 Eddy Covariance Network (UpCH4 v1.0): Model Development, Network Assessment, and Budget Comparison. *AGU Advances*, *4*(5), e2023AV000956. https://doi.org/10.1029/2023AV000956

Pastorello, G., Trotta, C., Canfora, E., Chu, H., Christianson, D., Cheah, Y.-W., Poindexter, C., Chen, J., Elbashandy, A., Humphrey, M., Isaac, P., Polidori, D., Reichstein, M., Ribeca, A., van Ingen, C., Vuichard, N., Zhang, L., Amiro, B., Ammann, C., … Papale, D. (2020). The FLUXNET2015 dataset and the ONEFlux processing pipeline for eddy covariance data. *Scientific Data*, *7*(1), Article 1. https://doi.org/10.1038/s41597-020-0534-3

Peltola, O., Vesala, T., Gao, Y., Räty, O., Alekseychik, P., Aurela, M., Chojnicki, B., Desai, A. R., Dolman, A. J., Euskirchen, E. S., Friborg, T., Göckede, M., Helbig, M., Humphreys, E., Jackson, R. B., Jocher, G., Joos, F., Klatt, J., Knox, S. H., … Aalto, T. (2019). Monthly gridded data product of northern wetland methane emissions based on upscaling eddy covariance observations. *Earth System Science Data*, *11*(3), 1263–1289. https://doi.org/10.5194/essd-11-1263-2019

Reed, D. E., Frank, J. M., Ewers, B. E., & Desai, A. R. (2018). Time dependency of eddy covariance site energy balance. *Agricultural and Forest Meteorology*, *249*, 467–478. https://doi.org/10.1016/j.agrformet.2017.08.008

Simard, M., Pinto, N., Fisher, J. B., & Baccini, A. (2011). Mapping forest canopy height globally with spaceborne lidar. *Journal of Geophysical Research: Biogeosciences*, *116*(G4). https://doi.org/10.1029/2011JG001708

Wang, Y., Yuan, F., Arndt, K. A., Liu, J., He, L., Zuo, Y., Zona, D., Lipson, D. A., Oechel, W. C., Ricciuto, D. M., Wullschleger, S. D., Thornton, P. E., & Xu, X. (2022). Upscaling Methane Flux From Plot Level to Eddy Covariance Tower Domains in Five Alaskan Tundra Ecosystems. *Frontiers in Environmental Science*, *10*. https://www.frontiersin.org/articles/10.3389/fenvs.2022.939238

Zhang, C., Comas, X., & Brodylo, D. (2020). A Remote Sensing Technique to Upscale Methane Emission Flux in a Subtropical Peatland. *Journal of Geophysical Research: Biogeosciences*, *125*(10), e2020JG006002. https://doi.org/10.1029/2020JG006002

Zhang, Z., Bansal, S., Chang, K.-Y., Fluet-Chouinard, E., Delwiche, K., Goeckede, M., Gustafson, A., Knox, S., Leppänen, A., Liu, L., Liu, J., Malhotra, A., Markkanen, T., McNicol, G., Melton, J. R., Miller, P. A., Peng, C., Raivonen, M., Riley, W. J., … Poulter, B. (2023). Characterizing Performance of Freshwater Wetland Methane Models Across Time Scales at FLUXNET-CH4 Sites Using Wavelet Analyses. *Journal of Geophysical Research: Biogeosciences*, *128*(11), e2022JG007259. https://doi.org/10.1029/2022JG007259

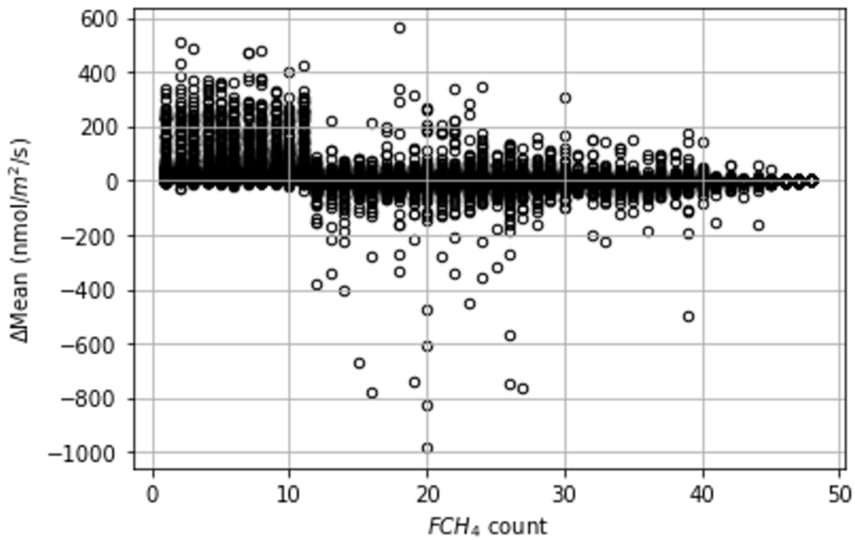

Fig. S1 The difference in daily mean fluxes between gap-filled data and original observations converged with the number of half-hourly observations in a day: On y-axis are gap-filled daily mean fluxs minus original observation daily means, on x-axis are half-hourly data counts of original observation in a day.

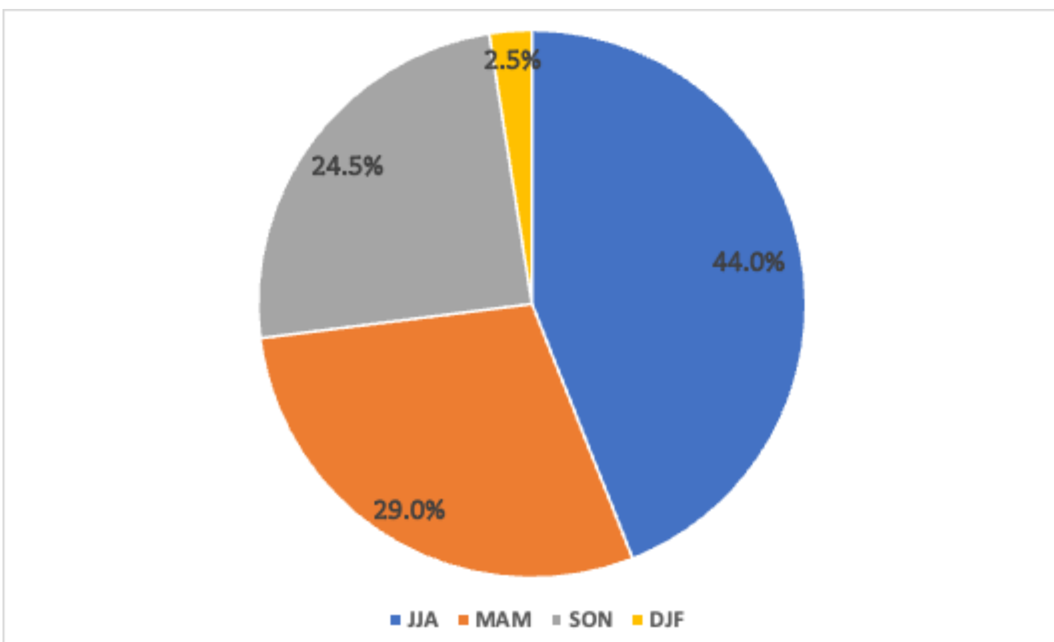

Fig. S2 Percentages of daily EC data in each season.

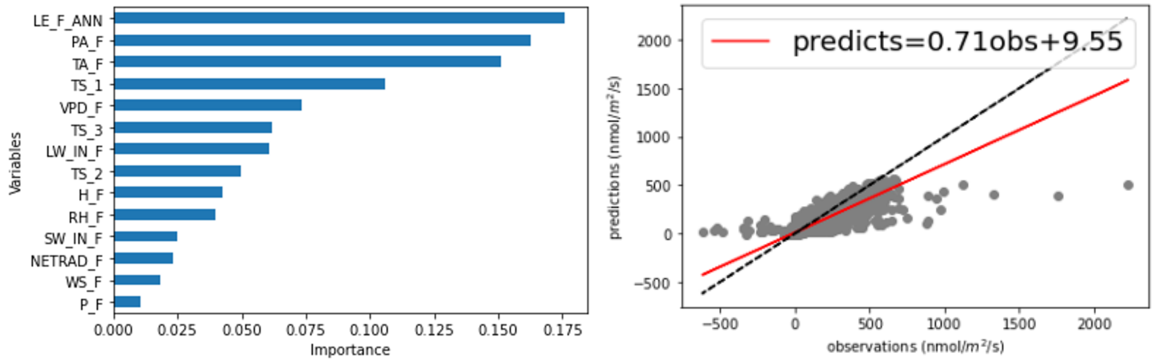

Fig. S3 Site level modeling for predictor variable selection: full predictor importance rank (left) and prediction-observation comparison (right).

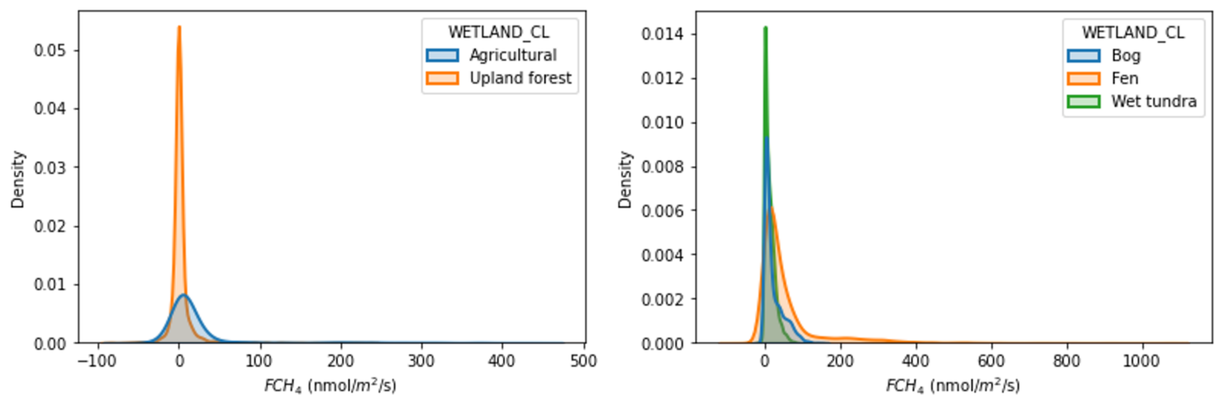

Fig. S4 Different distributions of daily mean CH_4 fluxes measured at EC sites between wetlands (fen 56±88 nmol m^{-2} s^{-1}, bog 22±26 nmol m^{-2} s^{-1}, wet tundra 13±14 nmol m^{-2} s^{-1}) and non-wetland land cover classes.

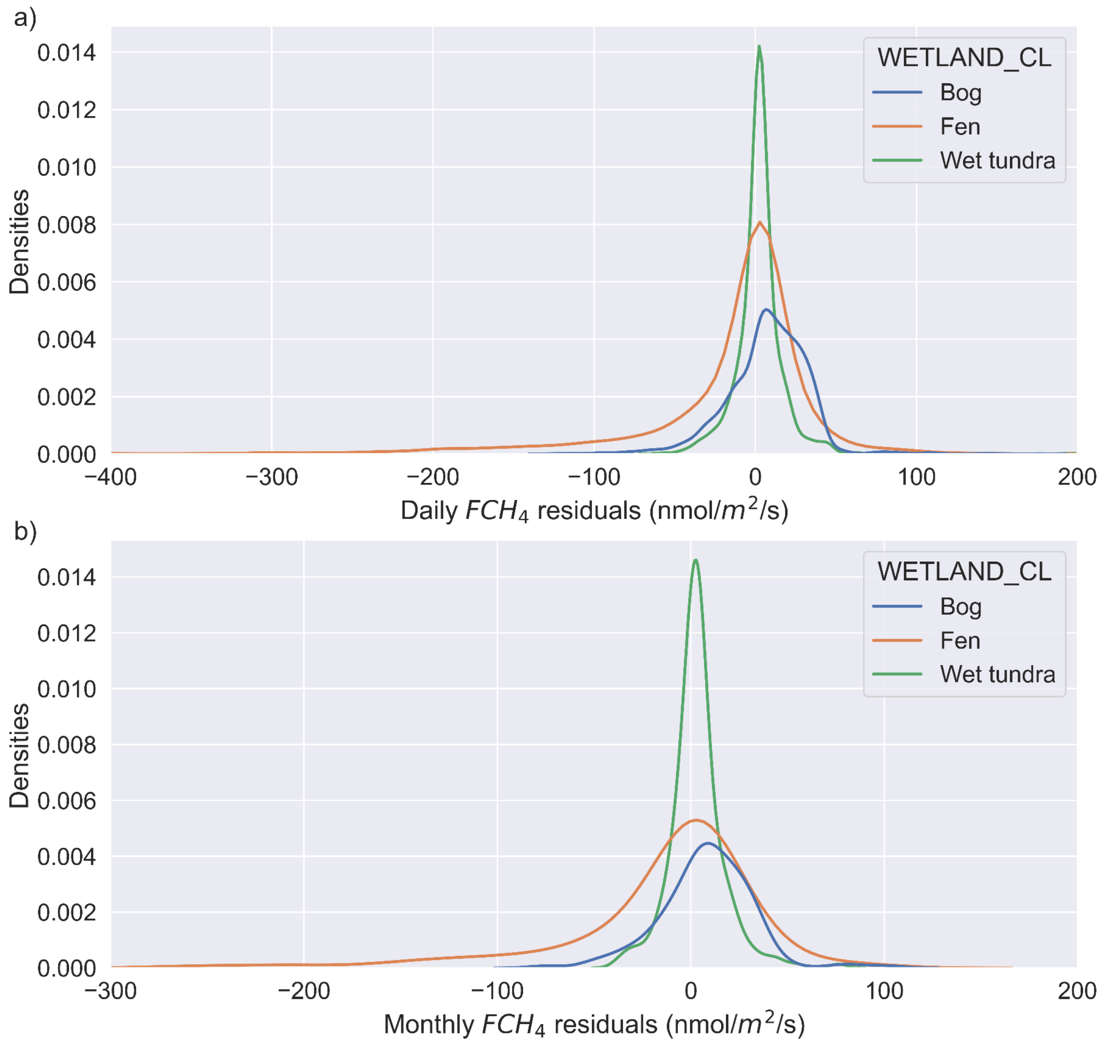

Fig. S5 Density distributions of prediction residuals of a) daily and b) monthly CH_4 fluxes by wetland types: fen (daily -17 ± 63 nmol m^{-2} s^{-1}, monthly -16 ± 61 nmol m^{-2} s^{-1}), bog (daily 8 ± 26 nmol m^{-2} s^{-1}, monthly 8 ± 24 nmol m^{-2} s^{-1}), wet tundra (daily 3 ± 9 nmol m^{-2} s^{-1}, monthly 3 ± 14 nmol m^{-2} s^{-1}).

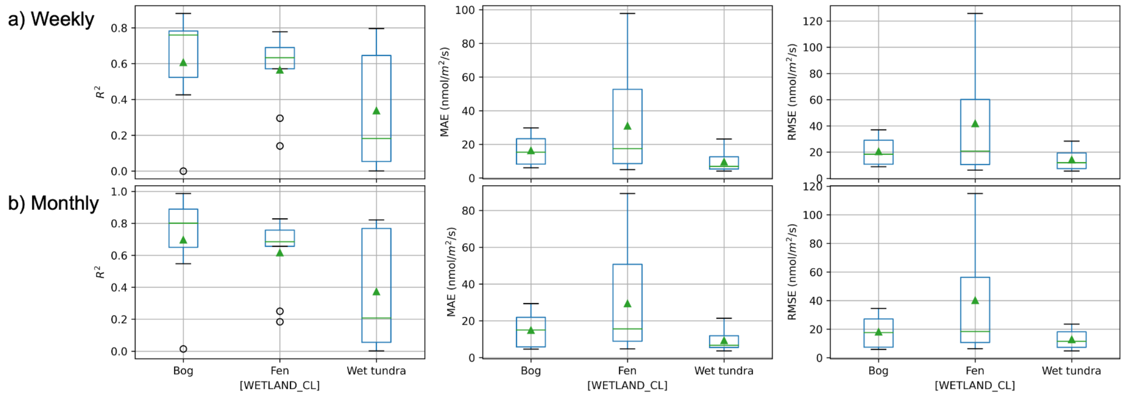

Fig. S6 Boxplots of R^2, MAE, and RMSE across validation sites by wetland types with mean values denoted in green triangles showing model predictive performance evaluation at a) weekly and b) monthly time steps.

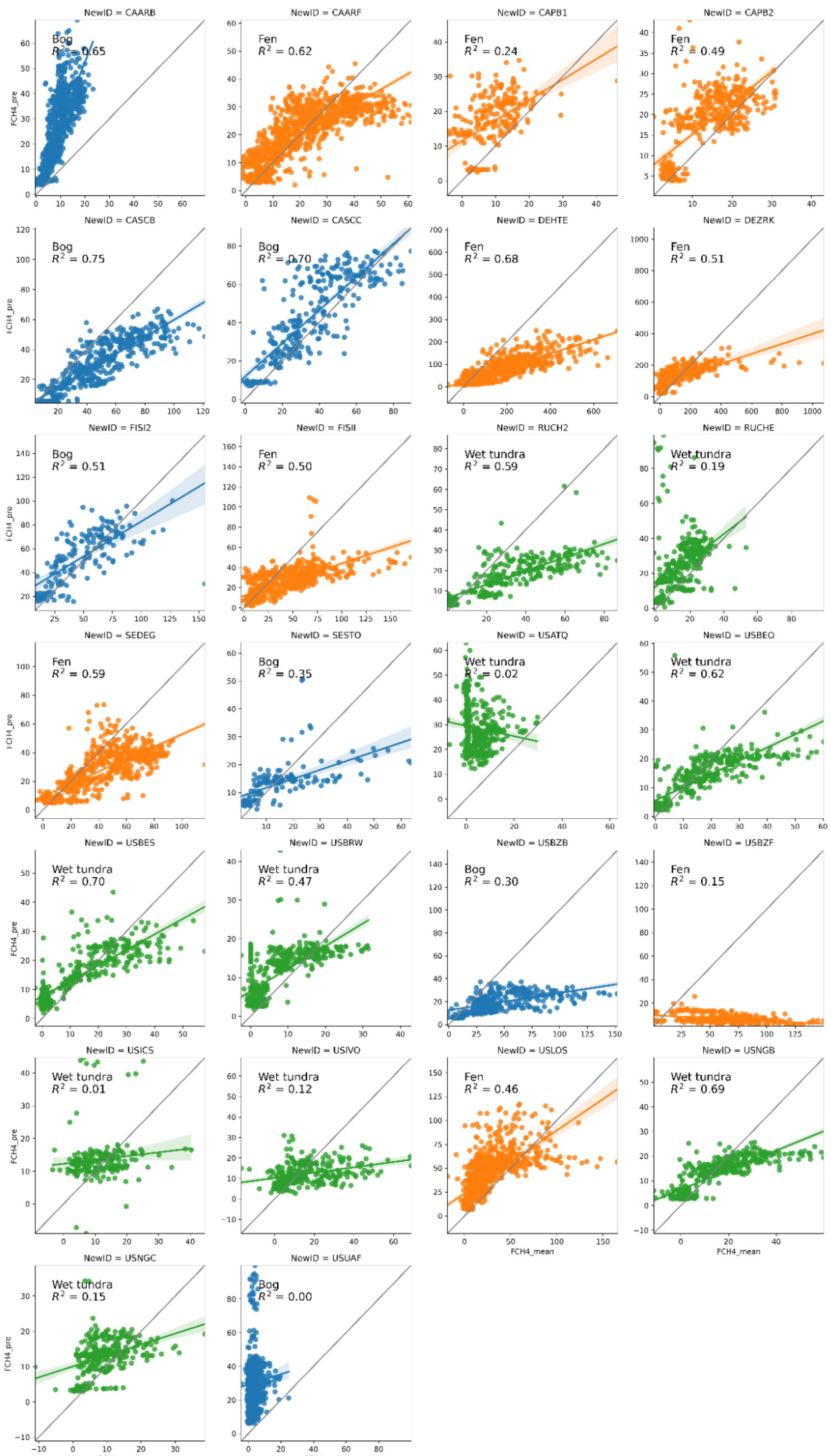

Fig. S7 Scatter plots of grid-level modeling by validation site

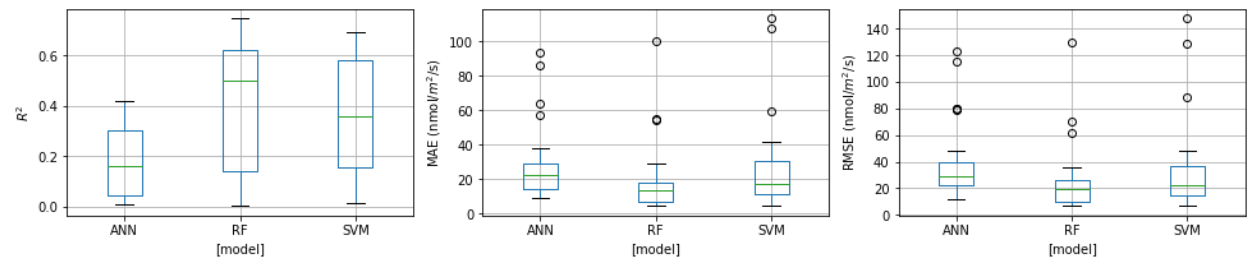

Fig. S8 Compare modeling predictive performance of ANN, RF, and SVM algorithms on evaluation metrics.

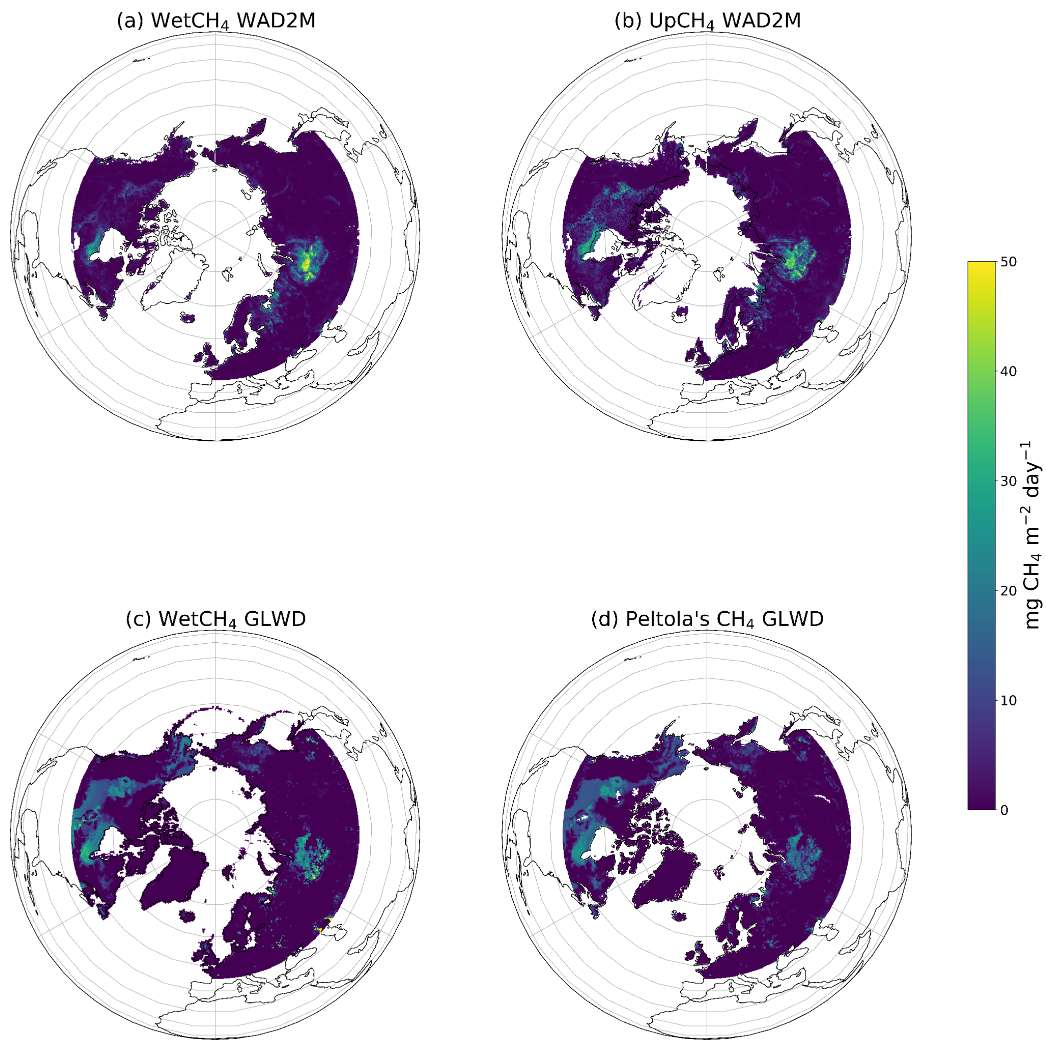

Fig. S9 Mean CH_4 fluxes of three ML-based upscaling products: (a) $WetCH_4$ and (b) $UpCH_4$ using WAD2M wetland area; (c) $WetCH_4$ and (d) CH_4 fluxes from Peltola et al. (2019) using GLWDv1 wetland area. $WetCH_4$ were averaged daily means 2016 - 2022, whereas $UpCH_4$ (2016-2018, McNicol et al., 2023) and Peltola et al. (2013-2014) were averaged monthly means.

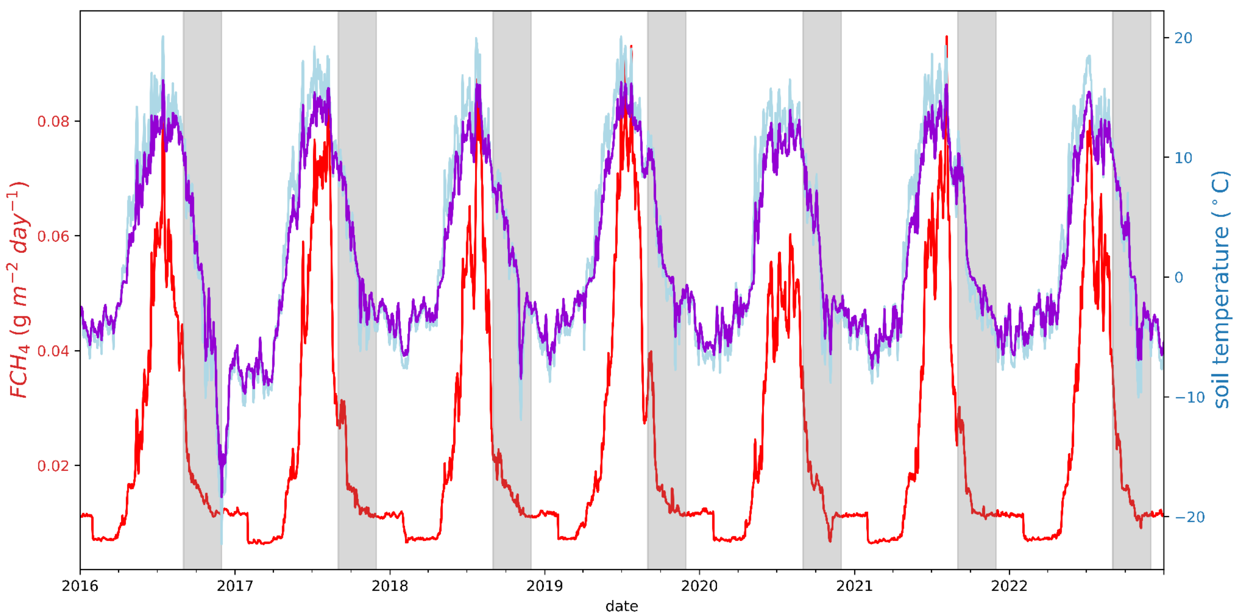

Fig. S10 Example of MERRA2 soil temperature at two different depths and modeled CH_4 fluxes at USUAF site. The discontinuity in soil temperature in late autumn (shaded) may hinder the model to capture the patterns of high emissions during zero curtain periods observed in Alaskan tundra.

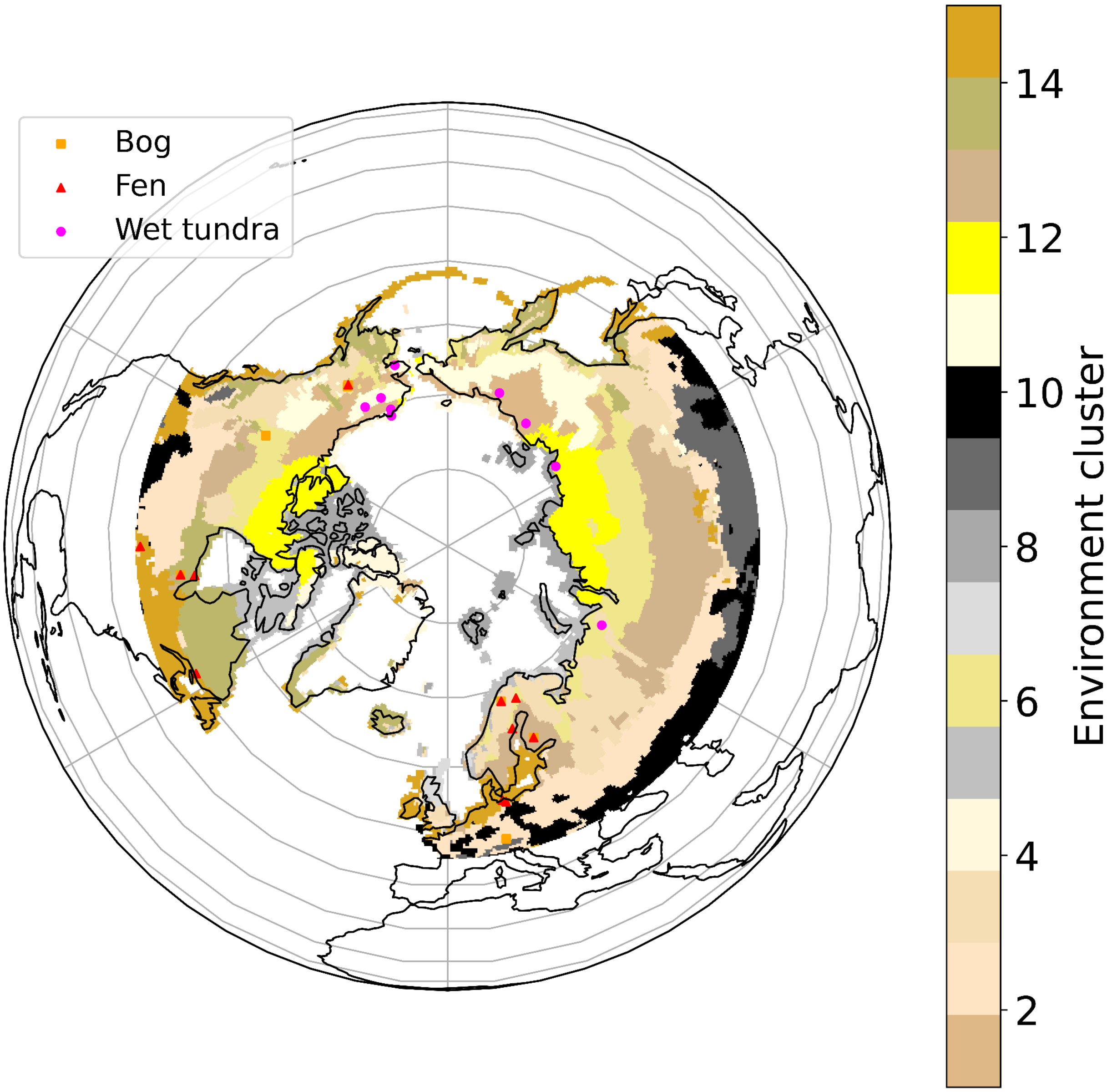

Fig. S11 Representativeness of 33 wetland EC sites to 15 environmental clusters: the clusters (5, 7, 8, 9, 10) in grayscale are underrepresented; the colored clusters (1, 2, 3, 4, 6, 11, 12, 13, 14, 15) are represented by wetland EC sites.

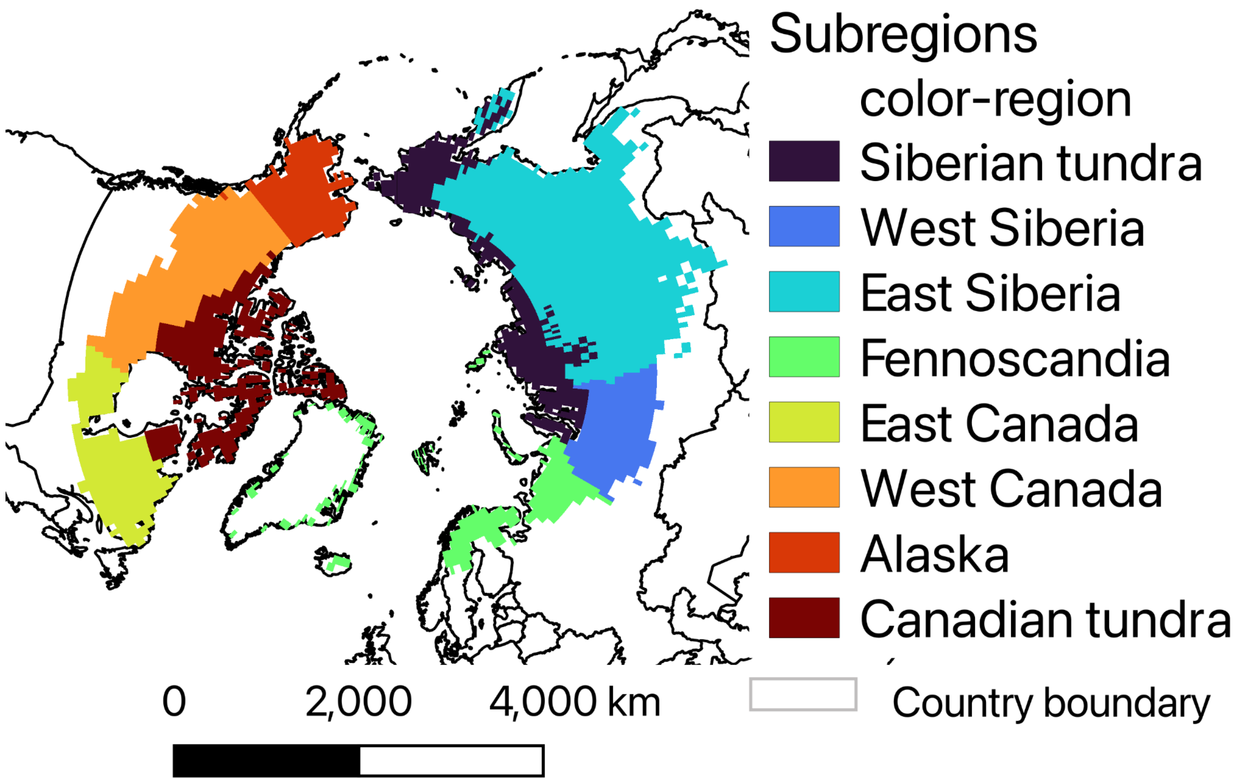

227
228 Fig. S12 Subregional extents in northern high latitudes.
229

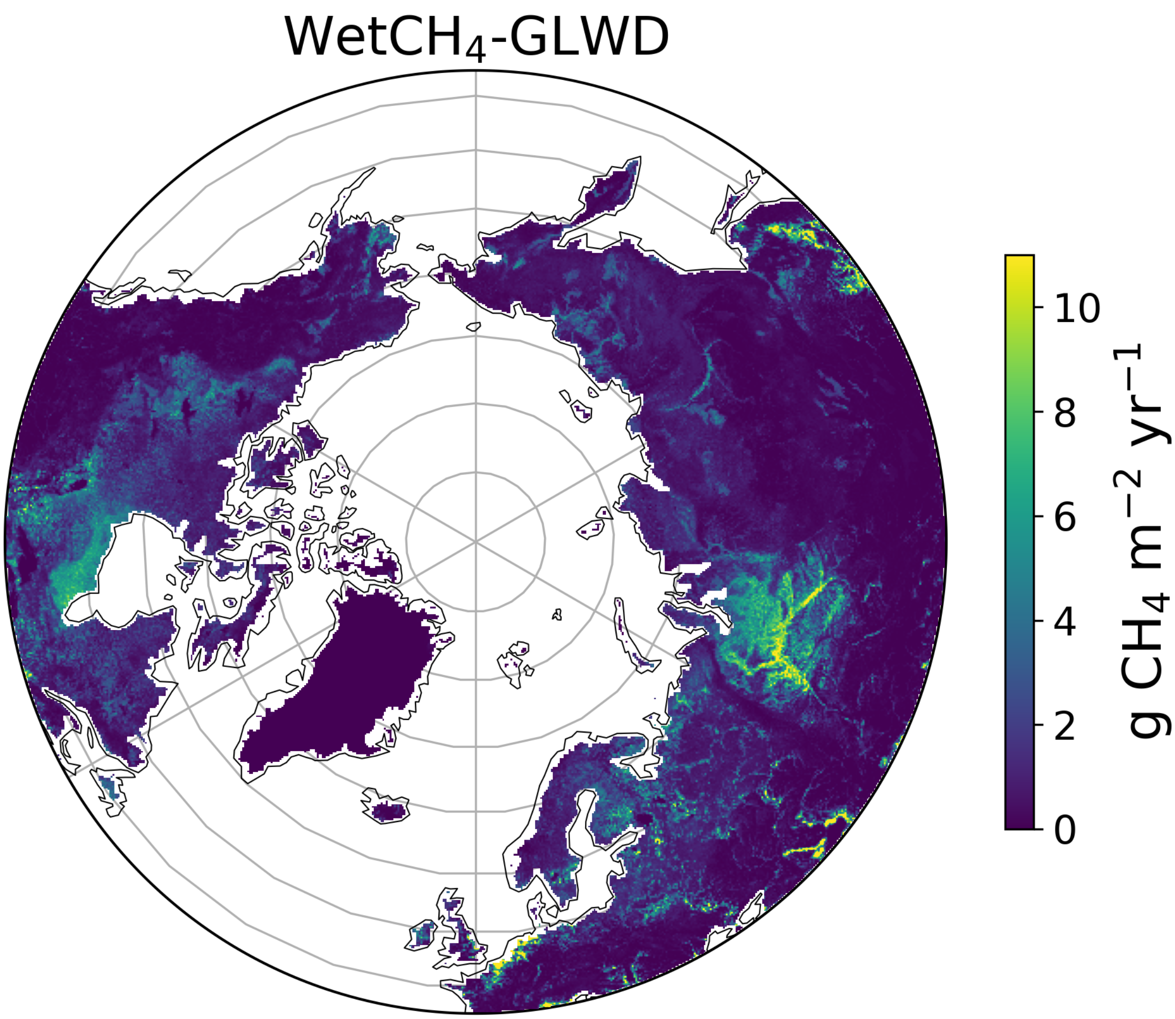

Fig. S13 WetCH$_4$ estimated mean annual wetland CH_4 emissions weighted with wetland areas from GLWD version 2.

Table S1. Comparison of ML-based wetland CH_4 upscaling products

Product	Peltola et al., 2019	McNicol et al., 2023	This study
Type	Freshwater wetland	Freshwater wetland	Freshwater wetland
Extent	Northern latitudes (>45° N)	Global	Northern latitudes (>45° N)
Period	2013-2014	2001-2018	2016-2022
Temporal resolution	Monthly	Weekly (modeled) Monthly (product)	Daily
Spatial resolution	0.25° - 0.5°	0.25°	0.098°

Table S2. Metadata of site identification, latitude, longitude, elevation from MERIT DEM (m), data start year, data end year, biome, land cover or wetland class, and data collection source. The metadata of the sites included in Fluxnet_CH_4 was collected from Delwiche et al. (2021) and the site websites.

Number	ID	LAT	LON	ELEVATION	Mean_Air_Temp_C	Mean_Precipitation_mm	YR_START	YR_END	BIOME_BAMS	WETLAND_CL	Daily counts after filtering	DJF_daily_counts	MAM_daily_counts	JJA_daily_counts	SON_daily_counts	Reference
1	CA-ARB	52.70	-83.95	94	5.5	719	2011	2019	Temperate	Bog	861	0	237	368	256	Todd, A. and Humphreys, E., 2022
2	CA-ARF	52.70	-83.96	92	5.5	719	2012	2019	Temperate	Fen	1083	0	295	460	328	Todd, A. and Humphreys, E., 2022
3	CA-PB1	54.94	-83.47	31	2.3	686	2016	2017	Temperate	Fen	243	0	54	92	97	Todd, A. and Humphreys, E., 2022
4	CA-PB2	54.94	-83.46	32	1.7	686	2017	2019	Temperate	Fen	429	0	93	181	155	Todd, A. and Humphreys, E., 2022
5	CA-SCB	61.31	-121.30	285	-2.8	388	2014	2018	Boreal Forests/Taiga	Bog	473	0	123	203	147	Delwiche et al., 2021
6	CA-SCC	61.31	-121.30	285	-2.8	387.6	2013	2017	Boreal Forests/Taiga	Bog	327	0	114	171	42	Delwiche et al., 2021
7	DE-HTE	54.21	12.18	0	9.2	645	2009	2018	Temperate	Fen	903	89	275	323	216	Delwiche et al., 2021
8	DE-ZRK	53.88	12.89	1	8.7	584	2013	2018	Temperate	Fen	457	26	158	144	129	Delwiche et al., 2021

9	FI-SI2	61.84	24.20	170	3.5	701	2012	2016	Boreal Forests/Taiga	Bog	181	0	0	108	73	Delwiche et al., 2021
10	FI-SII	61.83	24.19	170	3.5	701	2013	2018	Boreal Forests/Taiga	Fen	642	52	241	224	125	Delwiche et al., 2021
11	RU-CH2	68.62	161.35	5	-12.5	200	2014	2016	Boreal Forests/Taiga	Wet tundra	303	0	61	155	87	Delwiche et al., 2021
12	RU-CHE	68.61	161.34	4	-11	197	2014	2016	Boreal Forests/Taiga	Wet tundra	383	0	140	156	87	Delwiche et al., 2021
13	SE-DEG	64.18	19.56	267	1.2	523	2015	2018	Boreal Forests/Taiga	Fen	725	36	225	250	214	Delwiche et al., 2021
14	SE-STO	68.36	19.05	359	-0.14	322	2014	2016	Tundra	Bog	163	0	52	67	44	Delwiche et al., 2021
15	US-ATQ	70.47	-157.41	26	-9.7	93	2013	2018	Tundra	Wet tundra	382	7	153	168	54	Delwiche et al., 2021
16	US-BEO	71.28	-156.61	6	-11.3	72	2013	2018	Tundra	Wet tundra	407	0	111	223	73	Delwiche et al., 2021
17	US-BES	71.28	-156.60	5	-12	173	2013	2018	Tundra	Wet tundra	405	0	149	207	49	Delwiche et al., 2021
18	US-BRW	71.32	-156.61	7	-12.6	85	2013	2018	Tundra	Wet tundra	476	2	205	211	58	Delwiche et al., 2021
19	US-BZB	64.70	-148.32	120	-2.4	274	2014	2016	Boreal Forests/Taiga	Bog	347	0	111	160	76	Delwiche et al., 2021
20	US-	64.70	-148.31	142	-2.4	274	2014	2016	Boreal Forests/Taiga	Fen	308	0	78	166	64	Delwiche et al., 2021

	BZF															
21	US-ICS	68.61	-149.31	895	-7.4	318	2014	2016	Tundra	Wet tundra	198	0	6	147	45	Delwiche et al., 2021
22	US-IVO	68.49	-155.75	559	-8.28	304	2013	2018	Tundra	Wet tundra	318	5	100	162	51	Delwiche et al., 2021
23	US-LOS	46.08	-89.98	482	4.08	828	2014	2018	Temperate	Fen	989	69	291	336	293	Delwiche et al., 2021
24	US-NGB	71.28	-156.61	6	-11.27	171	2012	2019	Tundra	Wet tundra	413	0	117	240	56	Delwiche et al., 2021
25	US-NGC	64.86	-163.70	41	1.9	673	2017	2019	Boreal Forests/Taiga	Wet tundra	298	3	55	173	67	Delwiche et al., 2021
26	US-UAF	64.87	-147.86	161	-2.9	263	2011	2021	Boreal Forests/Taiga	Bog	904	28	181	457	238	Delwiche et al., 2021

Table S3. Annual emission budgets of northern wetlands (>45° N).

Tg CH_4 yr^{-1}	Annual mean	DJF mean	MAM mean	JJA mean	SON mean
$WetCH_4$_WAD2M	20.8 ± 2.1	1.4 ± 0.2	2.5 ± 0.3	12.4 ± 1.3	4.4 ± 0.4
$UpCH_4$_WAD2M	23.5 ± 5.8	1.4 ± 0.4	1.6 ± 0.5	10.8 ± 2.7	9.7 ± 2.2
$WetCH_4$_GIEMS2*	13.7 ± 1.5	0.2 ± 0.02	0.5 ± 0.1	9.2 ± 1.0	3.8 ± 0.4
$WetCH_4$_GLWDv1**	41.0 ± 4.5	4.0 ± 0.5	4.5 ± 0.5	23.2 ± 2.5	9.2 ± 0.9
$WetCH_4$_GLWDv2**	44.1 ± 1.7	4.4 ± 1.2	4.9 ± 0.2	24.3 ± 1.1	9.8 ± 0.3

Peltola et al._GLWDv1	37.6 ± 6.1	2.6 ± 0.4	5 ± 0.9	21.2 ± 3.5	9.2 ± 1.3
GCP ensemble mean	28.6 ± 21.6	1.3 ± 1.9	3.7 ± 3.0	17.1 ± 8.1	6.4 ± 4.4
WetCHARTs	29.5 ± 30	1.5 ± 2.2	3.8 ± 4.3	17.7 ± 12.7	6.4 ± 6.7
CarbonTracker-CH_4***	40.9	-1	2.7	34.1	5.2

*GIEMS2 represents the minimum extents of northern wetlands.
**GLWD provides a representation of the maximum extent of northern wetlands.
***These numbers are derived from CT natural microbial emissions, which include emissions from wetlands, river/lake/pond systems, and possibly wild animals (despite the small amount).